Am J Cancer Res 2018;8(8):1387-1402
www.ajcr.us /ISSN:2156-6976/ajcr0081833

Original Article

A novel circular RNA hsa_circ_0020123 exerts oncogenic properties through suppression of miR-144 in non-small cell lung cancer

Danhua Qu[1*], Bingdi Yan[1*], Rui Xin[2], Tiangang Ma[1]

Departments of [1]Pneumology, [2]Radiology, The 2nd Hospital Affiliated to Jilin University, Changchun 130021, Jilin Province, China. [*]Equal contributors.

Received June 19, 2018; Accepted July 11, 2018; Epub August 1, 2018; Published August 15, 2018

Abstract: Non-small cell lung cancer (NSCLC) is one of the leading causes of cancer-related death worldwide, while circulatory. Circular RNAs (circRNAs) are found to play important roles in cancer initiation and development. Herein, a novel functional circRNA hsa_circ_0020123 had been identified in NSCLC progression in this study, and elevated hsa_circ_0020123 expression could be observed in cancer tissues compared with that in matched normal lung tissues. Moreover, up-regulation of hsa_circ_0020123 was recognized to be closely associated with a poor differentiation degree, lymph node metastasis, a high TNM stage and dismal prognosis for NSCLC patients. Typically, knockdown of hsa_circ_0020123 could inhibit the NSCLC growth and metastasis both *in vitro* and *in vivo*, which could be reversed by the hsa_circ_0020123 overexpression. Importantly, miR-144 was identified as the hsa_circ_0020123-associated miRNA through performing RNA *in vivo* precipitation (RIP) in NSCLC cells using a biotin-labeled hsa_circ_0020123 probe. Besides, our results suggested that, miR-144 suppression had determined the oncogenic properties mediated by hsa_circ_0020123. In addition, hsa_circ_0020123 could upregulate ZEB1 and EZH2 through competitively binding with miR-144. Finally, the administration of hsa_circ_0020123 siRNA could suppress the growth and metastasis in NSCLC-bearing mice *in vivo*. In conclusion, the hsa_circ_0020123-miR-144-ZEB1/EZH2 axis is critical for NSCLC progression, which indicates that hsa_circ_0020123 is a potential target for NSCLC treatment.

Keywords: Circular RNA, miR-144, ceRNA, ZEB1, EZH2

Introduction

Lung cancer, one of the leading causes of cancer-related death worldwide, can be classified into non-small cell lung cancer (NSCLC) and small cell lung cancer (SCLC) [1, 2]. In recent years, progresses have been achieved in the diagnosis and treatments for NSCLC patients, including surgery, chemotherapy and radiotherapy. Nonetheless, most NSCLC patients are diagnosed at an advanced stage with metastasis, and the 5-year survival rate for NSCLC remains unsatisfactory [3]. Therefore, exploring the underlying molecular mechanism of NSCLC and identifying novel therapeutic targets is necessary for NSCLC treatment.

Numerous non-coding RNAs (ncRNAs) have already been identified thanks to the development in RNA deep sequencing technology. Circular RNAs (circRNAs), a novel class of ncRNA, are endogenous, abundant, conserved and jarless in mammalian cells, which have exerted crucial biological functions [4]. circRNAs display higher stability than the linear RNA, which can be ascribed to their structure of covalently closed continuous loop. Increasing evidence has demonstrated that circRNAs can sponge microRNAs and consequently regulate microRNAs activity [5]. In addition, circRNAs can also regulate the transcription of target genes through interaction with the RNA-binding proteins (RBPs), thus enhancing transcription and splicing competition [6-8]. circRNAs have been shown in previous studies to be differentially expressed in various diseases, which are closely correlated with the prognosis of diseases, such as diabetes mellitus [9], lupus nephritis [10]

and cancers [11]. For instance, circ-ITCH, a well-known cirRNA derived from several exons of itchy E3 ubiquitin protein ligase (ITCH), has been reported to be downregulated in bladder cancer and hepatocellular carcinoma (HCC) [12, 13]. Typically, circ-ITCH acts as a tumor suppressor to suppress tumor growth and metastasis. Mechanistically, circ-ITCH can upregulate the expression of p21 and PTEN through binding with miR-17 and miR-224 [12]. However, few circRNAs have been identified to be specifically related to the development and progression of NSCLC so far, except for the circ_0014130, circ_0007382 and circ_100876 [14-16]. Therefore, it is of urgent need to intensively investigate the potential roles of novel circRNAs in NSCLC.

Several abnormally expressed circRNAs have been found in a previous study in NSCLC tissue compared with the adjacent normal tissues through circRNAs microarray assay. Three circRNAs, including hsa_circ_0020123, hsa_circ_001235 and hsa_circ_0007385, have been recognized to be markedly upregulated in NSCLC tissues. Among them, hsa_circ_0007385 acts an oncogene, which can promote the aggressive phenotypes of NSCLC cells [15]. However, the pathological effects of hsa_circ_0020123 on NSCLC have not been well studied yet. Therefore, the current study was carried out aiming to define the relationship between the hsa_circ_0000064 expression and clinicopathological features of NSCLC patients, and to unveil the underlying mechanism of hsa_circ_0020123 in NSCLC tumorigenesis and progression.

Materials and methods

Tissues and cell lines

Eighty pairs of NSCLC tissue and adjacent normal lung tissue were excised from NSCLC patients, who underwent surgery without chemotherapy or radiotherapy at the 2nd Hospital Affiliated to Jilin University. The tissue samples were immediately frozen at -80°C until use. Informed consent was obtained from all patients. The experiments were approved by the Ethics Committee of the 2nd Hospital Affiliated to Jilin University. NSCLC cell lines PC9, H1573, A549, SK-MES-1, H1299, and Calu-3 were cultured in DMEM with 10% fetal bovine serum (Gibco, NY, USA). All of the cell lines were purchased from the Type Culture Collection of the Chinese Academy of Sciences (Shanghai, China).

Knockdown of hsa_circ_0020123

The siRNAs targeting hsa_circ_0020123 were synthesized and purchased from GenePharma (Shanghai, China). Scramble siRNA was taken as control. siRNAs (20 nmol/L) were transfected into the NSCLC cells using Lipofectamine 2000 (Invitrogen) according to the manufacturer's instructions. To construct stable knockdown hsa_circ_0020123 stable knockdown of A549 cells, A549 cells were infected with lentivirus expressing hsa_circ_0020123 shRNA by using 8 μg/mL polybrene. Stable cells were selected by selected in 1 μg/mL puromycin for two weeks.

Overexpression of hsa_circ_0020123

The sequence of hsa_circ_0020123 was amplified and cloned into circRNA overexpression vector pcD-ciR (Geneseed). The expression efficiency was detected by qRT-PCR after transfection. Stable cells were selected by selected in 1 μg/mL puromycin for two weeks.

RNA extraction and quantitative real-time PCR (qRT-PCR)

Total RNA from the tissue samples or cells was isolated using the Trizol reagent (Invitrogen, Carlsbad, CA, USA) according to the manufacturer's instructions. qRT-PCR was performed using Hieff™ qPCR SYBR Green Master Mix in the StepOne Plus instrument according to the manufacturer's instructions.

RNA in vivo precipitation

Biotin-labeled hsa_circ_0020123 probe was synthesized by Sangon Biotech, and the RNA in vivo precipitation assay was performed as previously described [17]. hsa_circ_0020123-overexpressing NSCLC cells were fixed by 1% formaldehyde for 10 minutes, lysed, and sonicated. After centrifugation, 50 μL of the supernatant was retained as input and the remaining part was incubated with a hsa_circ_0020123-specific probesstreptavidin dynabeads (Invitrogen) mixture overnight at 30°C. On the next day, a dynabeads-probes-circRNAs mixture was washed and incubated with 200 μL of

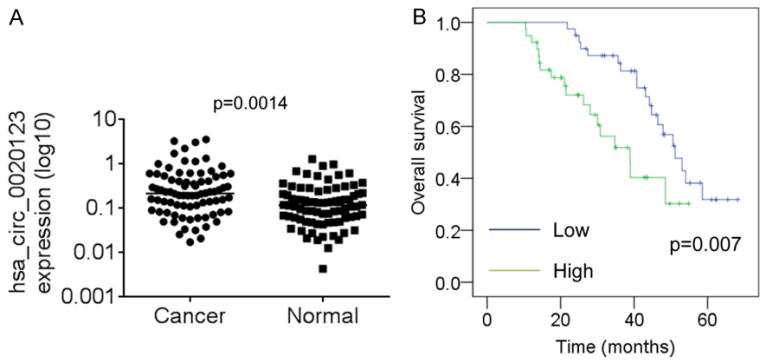

Figure 1. Upregulation of hsa_circ_0020123 expression is associated with poor prognosis of NSCLC patients. A. The hsa_circ_0020123 expression levels in 80 pairs of NSCLC and adjacent normal lung tissues were detected by qRT-PCR. B. The prognosis of NSCLC patients with different expression level of hsa_circ_0020123 was examined by Kaplan-Meier curves and log-rank test. The median of hsa_circ_0020123 expression in NSCLC tissues was taken as the cutoff. Low expression of hsa_circ_0020123 in 40 patients was classified as values below the 50th percentile. High hsa_circ_0020123 expression in 40 patients was classified as values at or above the 50th percentile.

lysis buffer and proteinase K to reverse the formaldehyde cross-linking. Finally, the mixture was added with TRIzol for RNA extraction and detection.

Transcriptome microarray analysis

The general profiles of human mRNA transcripts from the control and hsa_circ_0020123 knockdown cells were detected using the Arraystar Human mRNA Microarray. Array images were analyzed by Agilent Feature Extraction software. Differentially expressed genes were identified through the random variance model. A *P* value was calculated using the paired t-test. The threshold set for up- and down-regulated genes was a fold change ≥2.0 and a *P* value <0.05.

In vivo xenograft experiments

Six to eight week old male nude mice were used for the xenograft assays. NSCLC cells were trypsinized and harvested in PBS, then a total volume of 0.1 ml PBS containing 1×10^6 cells were injected subcutaneously into the flanks of the animals. Approximately 12 days later, tumors were detectable and tumor size was measured using a vernier caliper. Tumor volumes were calculated. A tail vein injection model was used for lung colonization assays. NSCLC cells were suspended in 0.1 ml PBS and intravenously injected via lateral tail veins of the mice. The mice were sacrificed 8 weeks later, and the lung metastases were analyzed histopathologically.

CCK-8 assay

Proliferation of NSCLC cells was performed using CCK-8 assay kit (Dojindo, Japan) according to manufacturer's instructions. NSCLC cells were seeded in 96-well plate at density of 1×10^3 per well. Cells were then added to 10 μl CCK-8 solution at 37°C for 90 min and incubated at 37°C. The absorbance was measured at 450 nm. All experiments were repeated at three times.

Apoptosis assay

Cells was collected 96 hours after incubation and stained for Annexin V. After incubation with FITC staining in dark for 20 minutes, FACS was performed to detect the peak of apoptosis cells which showed more ration of intensity.

Migration and invasion assay

Transwell assay was performed to measure migration and invasion. NSCLC cells (5×10^4) in 200 μL of serum-free medium were added to the upper chamber coated with or without 50 μL Matrigel (BD Biosciences, Franklin Lakes, NJ, USA) for 24 h. The lower chamber was added with medium containing 10% FBS. After incubation, the migrated and invaded cells on the lower membrane surface were removed with a cotton swab, and fixed with 95% ethanol and stained with 0.2% crystal violet solution (Sigma) and counted.

Dual-luciferase assay

The putative binding sites of miR-144 and hsa_circ_0020123 were subcloned into pmirGLO luciferase promoter plasmid (Promega, Madison, WI, USA). HEK-293T cells were transfected with luciferase reporter vector and miR-144 using Lipofectamine 2000 (Invitrogen). Luciferase and Renilla signal was measured 48 h after transfection using the Dual-Luciferase Reporter Assay System (Promega).

Table 1. The correlation between hsa_circ_0020123 and clinicopathlogical features of NSCLC patients

Characteristics	hsa_circ_0020123		*P*-Value
	Low	High	
Gender			
Male	25	24	0.818
Female	15	16	
Age			
<55	15	17	0.648
≥55	25	23	
T status			
T1-2	26	17	0.044
T3-4	14	23	
N status			
N0	22	12	0.024
N1/2	18	28	
Histological grade			
Well and moderately	26	15	0.014
Poorly and others	14	25	
Lymphatic metastasis			
Negative	25	14	0.014
Positive	15	26	

The median of hsa_circ_0020123 expression in NSCLC tissues was taken as the cutoff. Low expression of hsa_circ_0020123 in 40 patients was classified as values below the 50th percentile. High hsa_circ_0020123 expression in 40 patients was classified as values at or above the 50th percentile.

Statistical analysis

All results are expressed as the mean ± SD. All statistical data were analyzed using SPSS software (version 19.0). The difference between two groups was analyzed by the Student t test. The correlations between expression levels of hsa_circ_0020123 and clinicopathological features of NSCLC patients were analyzed by Chi-square test. P<0.05 was considered to be statistically significant.

Results

Upregulation of hsa_circ_0020123 expression is associated with the dismal prognosis for NSCLC patients

hsa_circ_0020123 expression in eighty NSCLC tissues and matched adjacent normal lung tissues was first detected through qRT-PCR. The results had revealed higher hsa_circ_0020123 expression in cancer tissues than in matched normal tissues (**Figure 1A**). Besides, patients were further classified into two groups, namely, the low-level and high-level groups, based on the median value of hsa_circ_0020123 expression in NSCLC tissues, so as to analyze the correlation between hsa_circ_0020123 expression and clinicopathological features of NSCLC patients. As shown in **Table 1**, patients with higher hsa_circ_0020123 expression level were associated with a poorer differentiation degree, lymph node metastasis and a higher TNM stage than those with low hsa_circ_0020123 expression level. Meanwhile, no significant correlations were observed between hsa_circ_0020123 expression and age or gender. Moreover, the relationship between hsa_circ_0020123 expression and the prognosis for NSCLC patients were also analyzed. The Kaplan-Meier survival curves demonstrated that NSCLC patients with higher hsa_circ_0020123 expression level had a shorter overall survival (OS) rate than that in the low-level group (**Figure 1B**). These results suggested that upregulation of hsa_circ_0020123 might serve as an oncogene for NSCLC progression.

hsa_circ_0020123 promotes the proliferation while inhibits the apoptosis of NSCLC cells in vitro

Subsequently, the role of hsa_circ_0020123 in NSCLC progression was investigated. hsa_circ_0020123 expression in 6 NSCLC cell lines were checked, including PC9, H1573, A549, SK-MES-1, H1299 and Calu-3 cells, so as to select the NSCLC cell lines used for loss- or gain-of-function assays. Our findings suggested that PC9 and A549 cells had higher hsa_circ_0020123 expression levels, while H1299 and Calu-3 cells had expressed lower levels of hsa_circ_0020123 (**Figure 2A**). Therefore, PC9 and A549 cells were selected for the knockdown of hsa_circ_0020123, whereas H1299 and Calu-3 cells were chosen for the overexpression of hsa_circ_0020123. At the same time, siRNA against hsa_circ_0020123 was constructed to target the back-splicing region of hsa_circ_0020123 for silencing. Subsequently, hsa_circ_0020123 siRNA was transfected into PC9 and A549 cells, and the knockdown efficiencies were detected using qRT-PCR (**Figure 2B**). Moreover, pCD-hsa_circ_0020123 plasmid was co-transfected with the circular

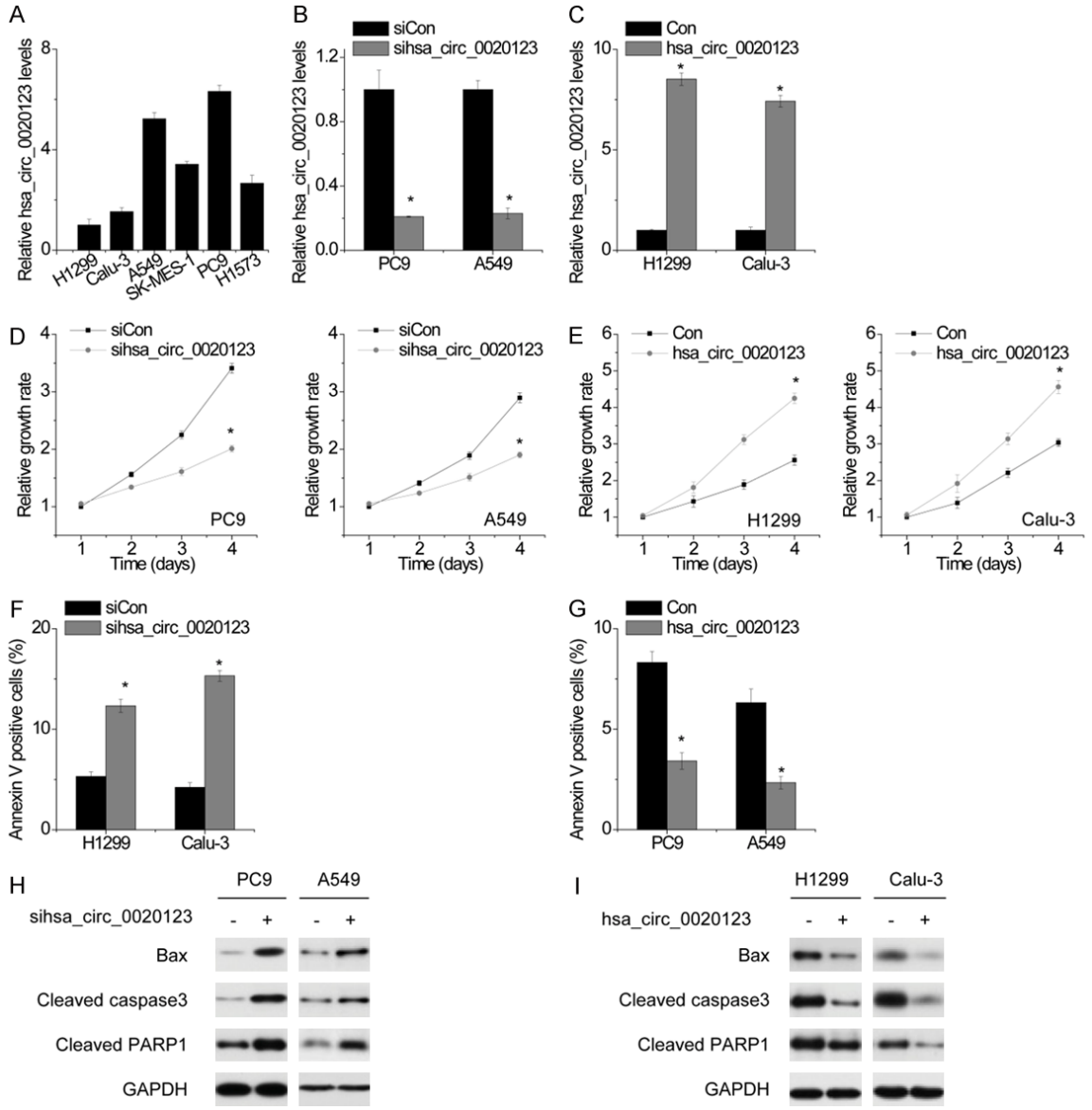

Figure 2. hsa_circ_0020123 promotes the proliferation and inhibits the apoptosis of NSCLC cells *in vitro*. (A) The hsa_circ_0020123 expression levels in different NSCLC cell lines were examined by qRT-PCR. (B) Control or hsa_circ_0020123 siRNAs were transfected into PC9 and A549 cells, and the hsa_circ_0020123 expression was detected by qRT-PCR. (C) Empty vector or full-length hsa_circ_0020123 were transfected into H1299 and Calu-3 cells, and the hsa_circ_0020123 expression was detected by qRT-PCR. (D) The effect of hsa_circ_0020123 knockdown on the proliferation of PC9 and A549 cells was detected by CCK-8 assay. (E) The effect of hsa_circ_0020123 overexpression on the proliferation of H1299 and Calu-3 cells was detected by CCK-8 assay. (F) PC9 and A549 cells with silenced hsa_circ_0020123 expression were stained with a combination of annexin V and 7-AAD and analyzed by FACS. Cells positive for annexin V staining were counted as apoptotic cells, and the percentage of apoptotic cells is shown. (G) H1299 and Calu-3 cells with hsa_circ_0020123 overexpression were stained with a combination of annexin V and 7-AAD and analyzed by FACS. Cells positive for annexin V staining were counted as apoptotic cells, and the percentage of apoptotic cells is shown. (H and I) Western blot was performed to detect the apoptosis markers in NSCLC cells with hsa_circ_0020123 knockdown (H) or overexpression (I). *P<0.05.

frame into H1299 and Calu-3 cells, the results of which demonstrated that hsa_circ_0020123 could be evidently upregulated in these two NSCLC cell lines (**Figure 2C**). CCK-8 assays showed that depletion of hsa_circ_0020123 could dramatically suppress the proliferation of PC9 and A549 cells (**Figure 2D**). In contrast, overexpression of hsa_circ_0020123

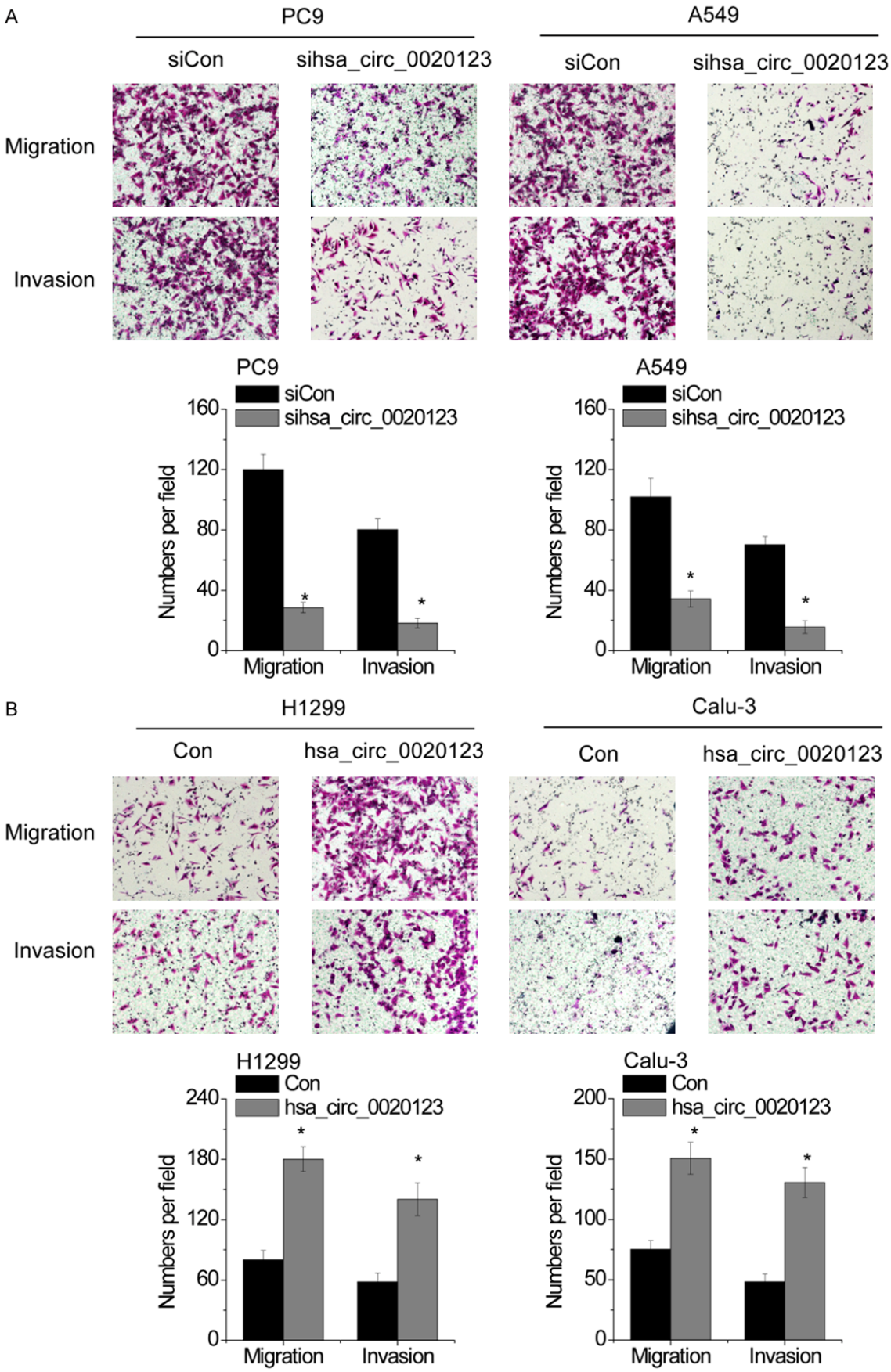
A
PC9
A549
siCon
sihsa_circ_0020123
siCon
sihsa_circ_0020123
Migration
Invasion
PC9
siCon
sihsa_circ_0020123
Numbers per field
160
120
80
40
0
*
*
Migration
Invasion
A549
siCon
sihsa_circ_0020123
Numbers per field
160
120
80
40
0
*
*
Migration
Invasion
B
H1299
Calu-3
Con
hsa_circ_0020123
Con
hsa_circ_0020123
Migration
Invasion
H1299
Con
hsa_circ_0020123
Numbers per field
240
180
120
60
0
*
*
Migration
Invasion
Calu-3
Con
hsa_circ_0020123
Numbers per field
200
150
100
50
0
*
*
Migration
Invasion

Figure 3. hsa_circ_0020123 enhances cell migration and invasion of NSCLC cells *in vitro*. A. The migration and invasive ability after knockdown of hsa_circ_0020123 in PC9 and A549 cells was assessed using transwell assays. B. The migration and invasive ability after knockdown of hsa_circ_0020123 in H1299 and Calu-3 cells was assessed using transwell assays. *P<0.05.

would enhance the proliferative capacity of both H1299 and Calu-3 cells (**Figure 2E**).

Afterwards, FACS analysis was also performed to detect the effect of hsa_circ_0020123 on the apoptosis of NSCLC cells. Our findings revealed that, compared with the control cells, the hsa_circ_0020123-silencing PC9 and A549 cells had notably higher percentages of Annexin V-positive cells (**Figure 2F**), whereas hsa_circ_0020123 overexpression would inhibit cell apoptosis (**Figure 2G**). Consistent with the FACS results, the well-defined apoptosis protein markers, Bax, cleaved PARP, and cleaved caspase 3, were remarkably upregulated after transfection with hsa_circ_0020123 siRNA (**Figure 2H**), while ectopic hsa_circ_0020123 expression showed an opposite effect (**Figure 2I**). Taken together, these data indicated that hsa_circ_0020123 could affect the proliferation and apoptosis of NSCLC cells.

hsa_circ_0020123 enhances the migration and invasion of NSCLC cells in vitro

To further investigate the role of hsa_circ_0020123 in the migration and invasion of NSCLC cells, Transwell assay was performed. The results revealed that, relative to the control group, hsa_circ_0007385 knockdown could suppress the migration and invasion of PC9 and A549 cells (**Figure 3A**). On the contrary, the migratory and invasive capacities of H1299 and Calu-3 cells were markedly promoted after the overexpression of hsa_circ_0020123 (**Figure 3B**).

hsa_circ_0020123 facilitates the growth and metastasis of NSCLC cells in vivo

Next, A549 cells with hsa_circ_002012 stable knockdown or control cells were injected into nude mice to determine whether hsa_circ_0020123 could affect NSCLC cell tumorigenesis *in vivo*. Our findings revealed that, tumors growing from cells with hsa_circ_0020123 stable knockdown were smaller than those from the control cells (**Figure 4A**). In the meantime, the tumor weight in the sh-hsa_circ_0020123 group was also dramatically lower than that in the control group (**Figure 4B**). Conversely, the hsa_circ_0020123 stable overexpressing H1299 cells or control cells were also injected into nude mice. Our results found that overexpression of hsa_circ_0020123 could significantly promote tumor growth in H1299 cells *in vivo* (**Figure 4C** and **4D**).

To evaluate whether hsa_circ_0020123 contributed to the progression of NSCLC *in vivo*, tail vein xenografts were performed, and the lung colonization was compared. Our results suggested that down-regulation of hsa_circ_0020123 in A549 cells would lead to reduced metastatic nodules in mice lungs compared with those in the control group (**Figure 4E** and **4F**). Moreover, the number of metastatic nodules in mice lungs in the H1299-hsa_circ_0020123 group was evidently increased relative to that in the H1299-control group (**Figure 4G** and **4H**).

hsa_circ_0020123 associates with miR-144

circRNA is found to serve as a miRNA sponge to regulate miRNA targets. As a result, the potential interactions between miRNAs and hsa_circ_0020123 were explored in this study. Through CircInteractome prediction (https://circinteractome.nia.nih.gov/), 101 miRNAs were predicated as the potential targets of hsa_circ_0020123 (data not shown). To confirm the association between hsa_circ_002012 and these miRNAs, RNA *in vivo* precipitation (RIP) was carried out using a hsa_circ_0020123-specific probe. Finally, 8 miRNAs were mainly screened and analyzed among these candidate miRNAs, whose expression and function had been implicated in NSCLC, including miR-95, miR-144, miR-21, miR-140, miR-183, miR-186, miR-375 and miR-488. Interestingly, results of RIP assay indicated a specific enrichment of hsa_circ_0020123 and miR-144 compared with the controls, whereas the other miRNAs were not enriched (**Figure 5A**). Besides, a dual-luciferase reporter system was employed for further confirmation. Afterwards, the alignment of potential binding site between hsa_circ_0020123 and miR-144 as well as its mutant type was constructed based on CircInter-

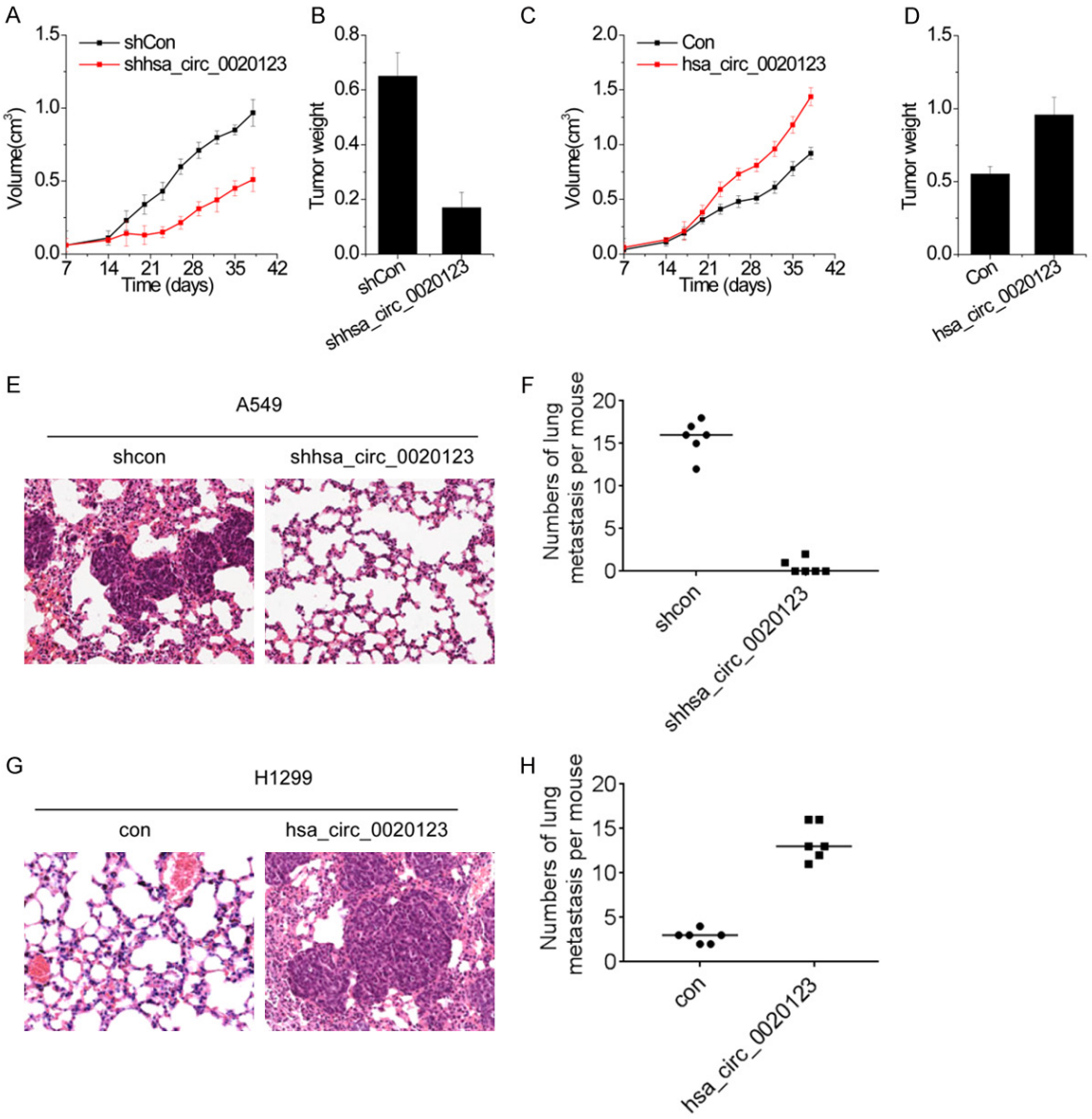

Figure 4. hsa_circ_0020123 facilitates growth and metastasis of NSCLC cells *in vivo*. (A and B) A549 cells stably expressing hsa_circ_0020123 shRNA or the negative control were used for *in vivo* tumorigenesis. Tumor growth curves after subcutaneous injection are shown. The tumor volumes were measured every 3 days after inoculation (A). Tumor weights are represented (B). (C and D) H1299 cells stably overexpressing hsa_circ_0020123 or the negative control were used for *in vivo* tumorigenesis. Tumor growth curves after subcutaneous injection are shown. The tumor volumes were measured every 3 days after inoculation (C). Tumor weights are represented (D). (E and F) Images showing representative hematoxylin and eosin staining of lung tissue samples from the A549 cells stably expressing hsa_circ_0020123 shRNA or the negative control (E). Number of lung metastatic foci observed in each group (F). (G and H) Images showing representative hematoxylin and eosin staining of lung tissue samples from the H1299 cells with overexpression of hsa_circ_0020123 or the negative control (G). Number of lung metastatic foci observed in each group (H).

actome prediction (**Figure 5B**). The results demonstrated that miR-144 mimics could reduce the luciferase activities of the wild-type pmirGLO-hsa_circ_0020123 reporter vector, which could not be observed in the empty vector or mutant reporter vector (**Figure 5C**). The AGO2-dependent manner is a common mechanism by which miRNAs represses the translation or RNA degradation of their targets. To determine whether hsa_circ_0020123 was regulated by miR-144 in this manner, anti-AGO2 RNA immunoprecipitation was conducted, the results of which found that hsa_circ_0020123 pull-down by AGO2 was specifically enriched in A549 cells

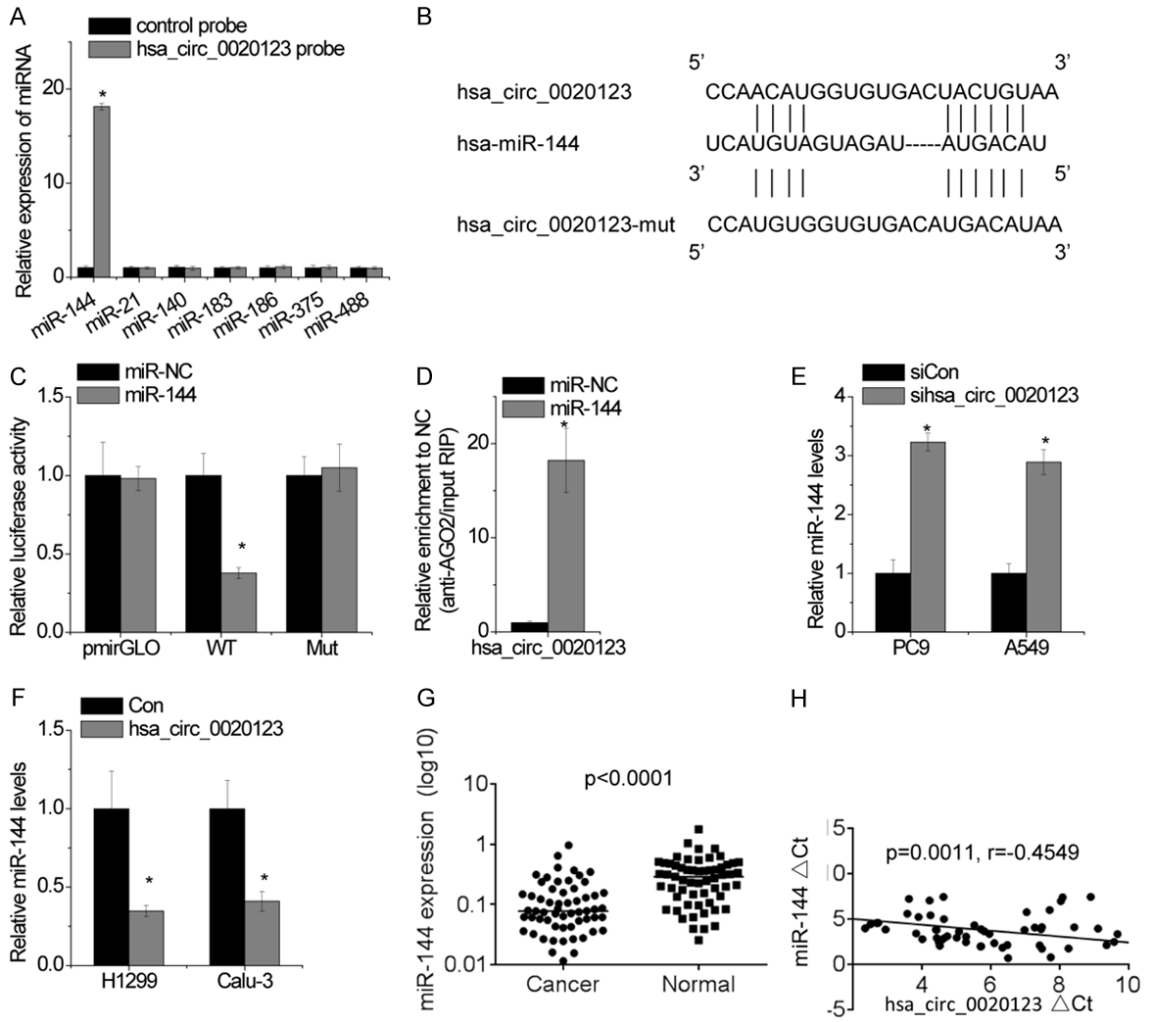

Figure 5. hsa_circ_0020123 associates with miR-144. A. The endogenous microRNA assoicated with hsa_circ_0020123 was examined by RNA *in vivo* precipitation (RIP) assay. B. The putative sequences of miR-144 and hsa_circ_0020123 with 10 paired nucleotides. C. Luciferase activity in H1299 cells cotransfected with miR-144 and luciferase reporters containing nothing, wild-type (WT) and mutant hsa_circ_0020123 (Mut) transcript. Data are presented as the relative ratio of firefly luciferase activity to renilla luciferase activity. D. The amout of hsa_circ_0020123 pulled down by AGO2 antibody was detected by RNA immunoprecipitation assay after miR-144 transfection. E. The miR-144 expression was determined by qRT-PCR in PC9 and A549 cells with hsa_circ_0020123 knockdown. F. The miR-144 expression was determined by qRT-PCR in H1299 and Calu-3 cells with hsa_circ_0020123 overexpression. G. The expression levels of miR-144 in 80 pairs of NSCLC and adjacent normal lung tissues. H. The correaltion between miR-144 and hsa_circ_0020123 expression in NSCLC tissues. *P<0.05.

transfected with miR-144 mimics (**Figure 5D**), indicating that miR-144 was a hsa_circ_0020123-targeting microRNA. Moreover, depletion of hsa_circ_0020123 could lead to increased miR-144 expression (**Figure 5E**), while ectopic hsa_circ_0020123 expression would downregulate miR-144 transcription (**Figure 5F**). Moreover, the pathological correlation between hsa_circ_0020123 and miR-144 expression was also explored. To this end, miR-144 expression in eighty NSCLC tissues and matched adjacent normal lung tissues were examined through qRT-PCR, which suggested that miR-144 was notably downregulated and was negatively correlated with hsa_circ_0020123 expression in NSCLC tissues (**Figure 5G** and **5H**).

hsa_circ_0020123 functions through suppressing miR-144

miR-144 exerts as a tumor suppressor in some cancers. Therefore, miR-144 was overexpressed in A549 cells and PC9 cells (**Figure 6A**).

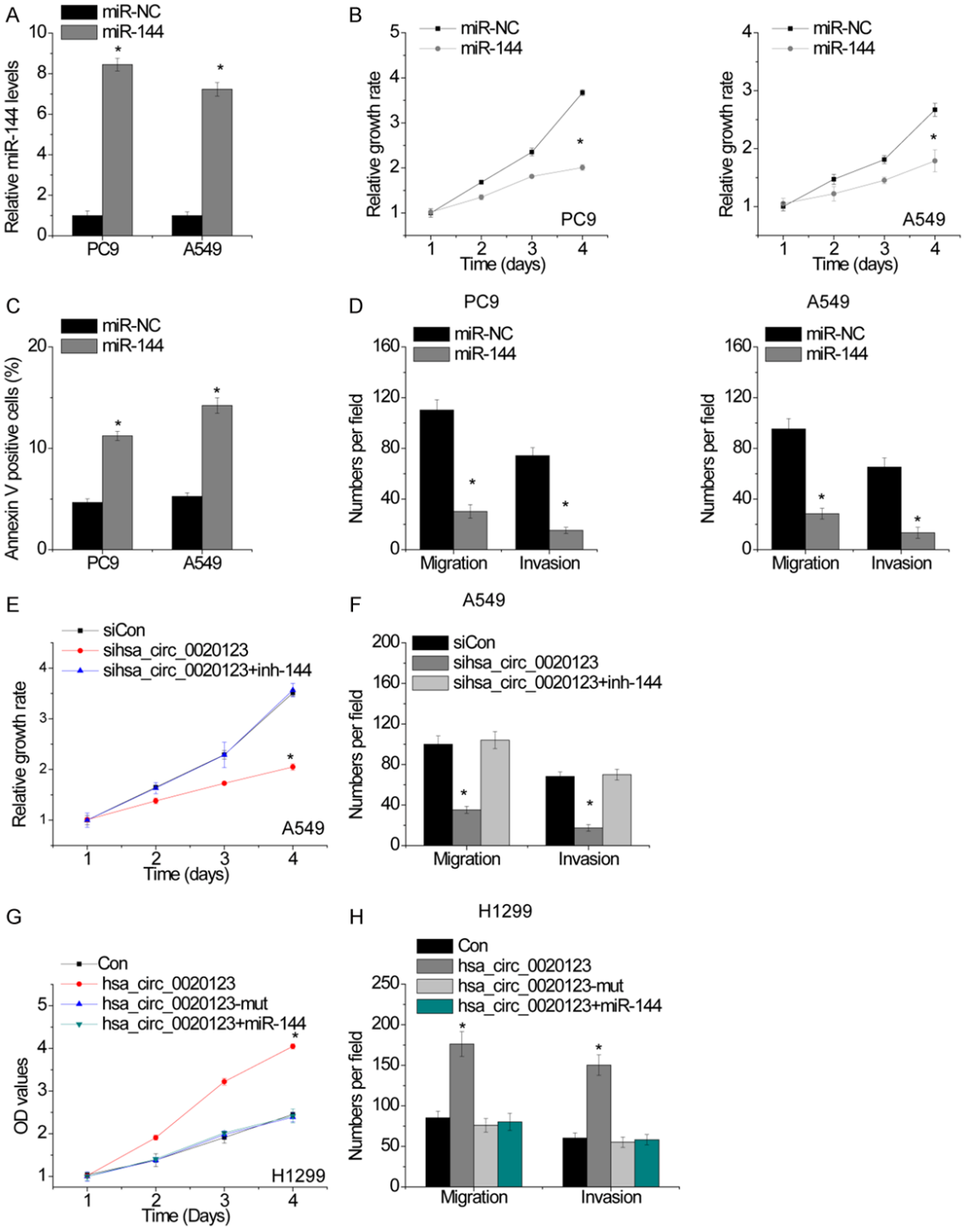

Figure 6. hsa_circ_0020123 functions through suppression miR-144. (A) The negative miRNA or miR-144 was transfected into PC9 and A549 cells, and the miR-144 expression was detected by qRT-PCR. (B) The effect of miR-144 overexpression on the proliferation of PC9 and A549 cells was detected by CCK-8 assay. (C) The effect of miR-144 overexpression on cell apoptosis was detected by FACS assay. Cells positive for annexin V staining were counted as apoptotic cells, and the percentage of apoptotic cells is shown. (D) The migration and invasive ability after transfection of miR-144 in PC9 and A549 cells was assessed using transwell assays. (E and F) The miR-144 inhibitor resuced the decrease of proliferation (E), migration and invasion (F) mediated by hsa_circ_0020123 knockdown in A549 cells. (G and H) The miR-144 overexpression abolished the proliferation (G), migration and invasion (H) enhanced by hsa_circ_0020123 overexpression in H1299 cells. *P<0.05.

Notably, miR-144 mimics could suppress the proliferation, migration and invasion, while induce the apoptosis of both A549 and PC9 cells (**Figure 6B-D**), which were similar to the phenotypes induced by hsa_circ_0020123 knockdown. Subsequently, rescue experiments were conducted to detect whether miR-144 was involved in the hsa_circ_0020123-induced malignant phenotypes. Our results indicated that miR-144 inhibitor could abrogate the effect of hsa_circ_0020123 on suppressing the proliferation, migration and invasion of A549 cells (**Figure 6E** and **6F**). Conversely, the overexpression of miR-144 could also reverse the elevated proliferation, migration and invasion induced by the overexpression of hsa_circ_0020123 (**Figure 6G** and **6H**); in contrast, hsa_circ_0020123 with mutations in miR-144 targeting sites (hsa_circ_0020123-mut) would not influence the malignant properties. Taken together, our results indicated that circRNA hsa_circ_0020123 could promote NSCLC progression by sponging miR-144.

hsa_circ_0020123 upregulates ZEB1 and EZH2 through competitively binding with miR-144

To further investigate the mechanism by which hsa_circ_0020123 exerted its oncogenic effect via miR-144, the transcriptome microarray analysis was carried out in control and hsa_circ_0020123 knockdown A549 cells (**Figure 7A**). Intriguingly, the well-known oncogenes EZH2 and ZEB1, which were targeted by miR-144 in cancer cells [17, 18], were found to be significantly downregulated by hsa_circ_0020123 siRNA. In addition, EZH2 and ZEB1 was targeted by miR-144 in cancer cells [18, 19]. Therefore, it was speculated that hsa_circ_0020123 could upregulate EZH2 and ZEB1 through acting as a competing endogenous RNA (ceRNA) for miR-144. Moreover, the overexpression of hsa_circ_0020123, but not the mutant, would increase the ZEB1 and EZH2 transcript levels (**Figure 7B**), which could be abrogated through the ectopic expression of miR-144. In contrast, the depletion of hsa_circ_0020123 decreased the ZEB1 and EZH2 levels (**Figure 7C**), which such decreases could be reversed through the inhibition of miR-144. These results were further confirmed by Western blotting (**Figure 7D** and **7E**).

To ascertain whether the observed effect depended on the regulation of ZEB1 and EZH2 3'UTR, the luciferase reporters gene assay containing either the ZEB1 or EZH2 3'UTR (pmirGLO-ZEB1 or pmirGLO-EZH2) was conducted. Specifically, the luciferase plasmid (pmirGLO-ZEB1, pmirGLO-EZH2, or the control reporter [pmirGLO]) was transfected into the NSCLC cells. The results indicated that, the overexpression of hsa_circ_0020123, but not the mutant, could enhance the luciferase activities of pmirGLO-ZEB1 and pmirGLO-EZH2, whereas such up-regulation could be abolished by the ectopic expression of miR-144 (**Figure 7F**). Reciprocally, depletion of hsa_circ_0020123 would decrease the luciferase activities of pmirGLO-ZEB1 and pmirGLO-EZH2, which could be rescued by miR-144 suppression (**Figure 7G**). In conclusion, these results suggested an important role of hsa_circ_0020123 in modulating ZEB1 and EZH2, which was achieved through competitively binding with miR-14.

Silencing hsa_circ_0020123 by siRNA delivery suppresses NSCLC growth and metastasis in vivo

Finally, the therapeutic potential of siRNA specifically targeting hsa_circ_0020123 was examined using a xenograft model. Briefly, A549 cells were injected subcutaneously into one flank of nude mice. Two weeks after cell injection, mice were randomly classified into two groups to receive either intraperitoneal injection of cholesterol-conjugated control scramble siRNA or hsa_circ_0020123 siRNA for 30 days. Our results suggested that xenograft tumors injected with hsa_circ_0020123 siRNA were associated with smaller mean volumes and weights than those injected with control siRNA (**Figure 8A** and **8B**).

Next, the therapeutic effect of hsa_circ_0020123 siRNA on NSCLC metastasis was also evaluated. Specifically, the A549 cells were injected into the tail vein of nude mice, followed by injection with control or hsa_circ_0020123 siRNA. The results showed that, compared with the control group, hsa_circ_0020123 siRNAs could dramatically inhibit the pulmonary metastasis (**Figure 8C**). Collectively, these results indicated that circRNA hsa_circ_0020123 might serve as a promising therapeutic target for NSCLC treatment.

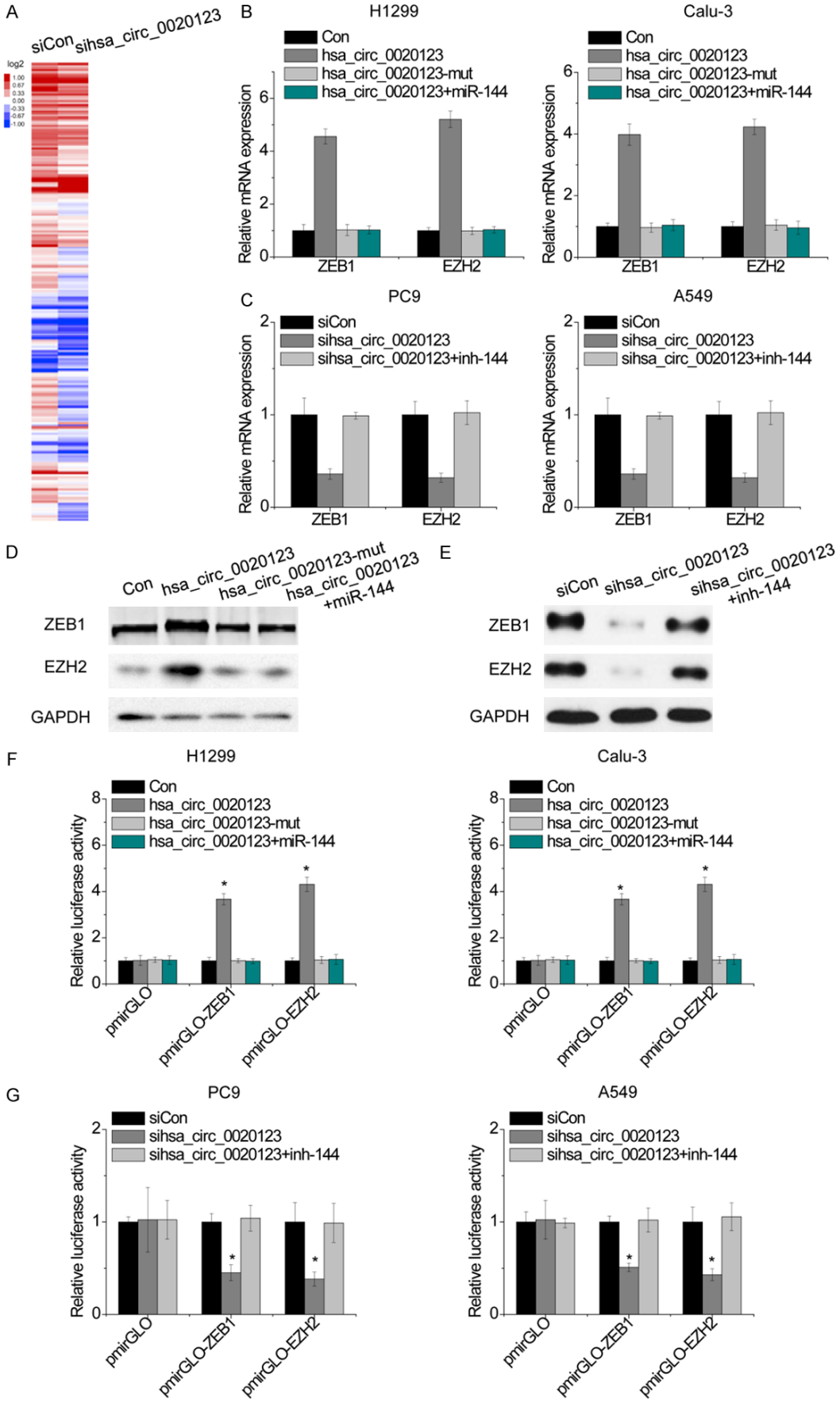
A
siCon
sihsa_circ_0020123
log2
B
H1299
Calu-3
Con
hsa_circ_0020123
hsa_circ_0020123-mut
hsa_circ_0020123+miR-144
Relative mRNA expression
ZEB1
EZH2
C
PC9
A549
siCon
sihsa_circ_0020123
sihsa_circ_0020123+inh-144
D
Con
hsa_circ_0020123
hsa_circ_0020123-mut
hsa_circ_0020123 +miR-144
ZEB1
EZH2
GAPDH
E
siCon
sihsa_circ_0020123
sihsa_circ_0020123 +inh-144
F
H1299
Calu-3
Relative luciferase activity
pmirGLO
pmirGLO-ZEB1
pmirGLO-EZH2
G
PC9
A549

Figure 7. hsa_circ_0020123 upregulates ZEB1 and EZH2. A. Hierarchically clustered heatmap of upregulated and downregulated genes in A549 cells after transfection with hsa_circ_0020123 or NC siRNAs. B. miR-144 was transfected into hsa_circ_0020123 or mutant hsa_circ_0020123 overexpressing H1299 and Calu-3 cells, and the mRNA levels of ZEB1 and EZH2 were detected by qRT-PCR. C. miR-144 inhibitor was transfected into hsa_circ_0020123 knockdown PC9 and A549 cells, and the mRNA levels of ZEB1 and EZH2 were detected by qRT-PCR. D. miR-144 abolished the upregulation of ZEB1 and EZH2 protein levels mediated by hsa_circ_0020123 overexpression in H1299 cells. E. miR-144 inhibitor abolished the downregulation of ZEB1 and EZH2 protein levels mediated by hsa_circ_0020123 knockdown in A549 cells. F. H1299 and Calu-3 cells with hsa_circ_0020123 overexpression were cotransfected with miR-144 and luciferase reporters containing ZEB1 3'UTR, EZH2 3'UTR or nothing. Luciferase activity was detected and the data are presented as the relative ratio of firefly luciferase activity to renilla luciferase activity. G. PC9 and A549 cells with hsa_circ_0020123 knockdown were cotransfected with miR-144 inhibitor and luciferase reporters containing ZEB1 3'UTR, EZH2 3'UTR or nothing. Luciferase activity was detected and the data are presented as the relative ratio of firefly luciferase activity to renilla luciferase activity. *P<0.05.

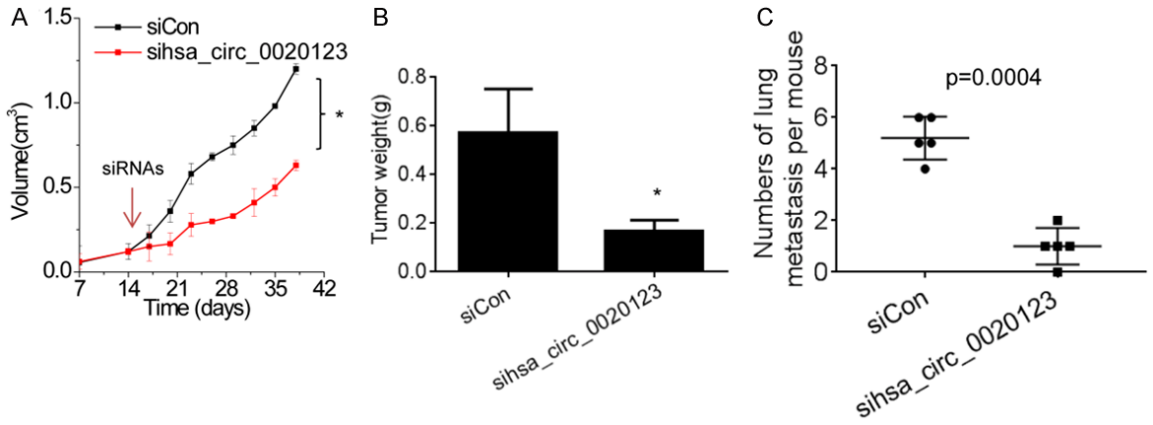

Figure 8. Silence of hsa_circ_0020123 by siRNA delivery suppresses NSCLC growth and metastasis *in vivo*. A. Tumor growth curves formed in nude mice injected subcutaneously with A549 cells treated with control and hsa_circ_0020123 siRNAs. B. Tumor weight was measured. C. The number of pulmonary metastasis in control and hsa_circ_0020123 siRNAs-treated mice. *P<0.05.

Discussion

CircRNAs are a type of novel non-coding RNAs closely associated with carcinogenesis and cancer progression, whose functional significance in different cancers has attracted extensive attention recently. Some existing studies have examined the circRNA expression profiles in NSCLC tissues; however, the exact function and mechanism of novel circRNAs remains unclear at present. Therefore, the current study aims to detect the expression of circRNA hsa_circ_0020123 in NSCLC tissues and reveal its functional role in NSCLC progression.

Previous studies have examined the differentially expressed circRNAs between NSCLC and matched normal lung tissues through RNA sequencing or chip microarray [14, 15]. Nonetheless, only a handful of circRNAs have been functionally identified. For instance, circRNA circMAN2B2 is highly expressed in NSCLC tissues, which can promote the proliferation and invasion of NSCLC tissues both in vivo and in vitro. Moreover, the oncogenic function of circMAN2B2 depends on the regulation of FOXK1 expression through sponging miR-1275 [20]. In the meantime, hsa_circ_0012673 is also found to be markedly up-regulated in NSCLC tissues, which is also closely correlated with a greater tumor size. Typically, hsa_circ_0012673 can regulate cell proliferation through sponging miR-22, which targets ErbB3 in NSCLC [21]. In the current study, we have identified a novel functional circRNA hsa_circ_0020123 in NSCLC. Our results suggest that hsa_circ_0020123 expression is notably upregulated in NSCLC tissues than in matched normal tissues. In addition, the higher hsa_circ_0020123 expression level is found to be closely associated with a poorer differentiation degree, lymph node metastasis, a higher TNM stage and worse prognosis for NSCLC patients. Besides, knockdown of hsa_circ_0020123 can suppress the proliferation, migration and invasion,

whereas induce the apoptosis in NSCLC cells. By contrast, overexpression of hsa_circ_0020123 can enhance the proliferative, migratory and invasive capacities of NSCLC cells. In addition, our *in vivo* assays using xenograft model also shows that siRNA specifically targeting hsa_circ_0020123 can remarkably suppress the growth and metastasis of NSCLC, indicating that hsa_circ_0020123 may be a potential therapeutic target of NSCLC.

The majority of circRNAs are primarily localized in the cytoplasm, which act as the miRNA sponges to regulate the expression of target miRNAs. By competing for miRNAs, circRNAs can regulate mRNA expression at post-transcriptional level [22]. miR-144 is a tumor suppressor miRNA in some cancers, including breast cancer, gastric cancer, cervical cancer and NSCLC [2, 23-25]. It is found to inhibit tumor growth and metastasis through targeting some well-known oncogenes, such as RUNX1, PIM1, E2F8, ZEB1, EZH2, ROCK1 and TIGAR [18, 19, 26-30]. On the other hand, the long non-coding RNAs (lncRNAs), such as CASC2, MALAT1 and TUG1, are demonstrated to be associated with miR-144 in facilitating tumorigenesis and cancer aggression [31-33]. However, no reports are available regarding the association between circRNAs and miR-144 so far. In the current study, results of RIP and luciferase reporter assays have revealed a direct interaction between hsa_circ_0020123 and miR-144. Furthermore, it is also discovered in the current study that, hsa_circ_0020123 can downregulate miR-144 expression and regulate miR-144 targets, including ZEB1 and EZH2. Besides, hsa_circ_0020123 is found to be negatively correlated with miR-144 expression in NSCLC tissues, which further supports that miR-144 is a bona fide target miRNA of hsa_circ_0020123. However, it remains to be further investigated about whether other miRNAs are involved in the hsa_circ_0020123-mediated aggressive phenotypes of NSCLC.

In conclusion, our findings reveal that hsa_circ_0020123 expression is markedly up-regulated in NSCLC tissues, which is also correlated with the dismal prognosis for NSCLC patients. Functionally and mechanistically, hsa_circ_0020123 can promote the proliferation, migration and invasion of NSCLC through sponging miR-144 and subsequently regulating its targets, indicating its oncogenic role in NSCLC progression. Moreover, the suppression of hsa_circ_0020123 silencing *in vivo* has indicated its potential for NSCLC-targeted therapy. Moreover, our data suggest that hsa_circ_0020123 may serve as a promising prognosis predictor and therapeutic target for NSCLC.

Disclosure of conflict of interest

None.

Address correspondence to: Dr. Rui Xin, Department of Radiology, The 2nd Hospital Affiliated to Jilin University, No. 218 Ziqiang Street, Nanguan District, Changchun 130021, Jilin Province, China. E-mail: xin-1017@163.com; Dr. Tiangang Ma, Department of Pneumology, The 2nd Hospital Affiliated to Jilin University, No. 218 Ziqiang Street, Nanguan District, Changchun 130021, Jilin Province, China. E-mail: matg2001@163.com

References

[1] Ferlay J, Soerjomataram I, Dikshit R, Eser S, Mathers C, Rebelo M, Parkin DM, Forman D and Bray F. Cancer incidence and mortality worldwide: sources, methods and major patterns in GLOBOCAN 2012. Int J Cancer 2015; 136: E359-386.

[2] Yin Y, Cai J, Meng F, Sui C and Jiang Y. MiR-144 suppresses proliferation, invasion, and migration of breast cancer cells through inhibiting CEP55. Cancer Biol Ther 2018; 19: 306-315.

[3] DeSantis CE, Lin CC, Mariotto AB, Siegel RL, Stein KD, Kramer JL, Alteri R, Robbins AS and Jemal A. Cancer treatment and survivorship statistics, 2014. CA Cancer J Clin 2014; 64: 252-271.

[4] Zhang M and Xin Y. Circular RNAs: a new frontier for cancer diagnosis and therapy. J Hematol Oncol 2018; 11: 21.

[5] Piwecka M, Glazar P, Hernandez-Miranda LR, Memczak S, Wolf SA, Rybak-Wolf A, Filipchyk A, Klironomos F, Cerda Jara CA, Fenske P, Trimbuch T, Zywitza V, Plass M, Schreyer L, Ayoub S, Kocks C, Kuhn R, Rosenmund C, Birchmeier C and Rajewsky N. Loss of a mammalian circular RNA locus causes miRNA deregulation and affects brain function. Science 2017; 357.

[6] Li Z, Huang C, Bao C, Chen L, Lin M, Wang X, Zhong G, Yu B, Hu W, Dai L, Zhu P, Chang Z, Wu Q, Zhao Y, Jia Y, Xu P, Liu H and Shan G. Exon-intron circular RNAs regulate transcription in the nucleus. Nat Struct Mol Biol 2015; 22: 256-264.

[7] Ashwal-Fluss R, Meyer M, Pamudurti NR, Ivanov A, Bartok O, Hanan M, Evantal N, Memc-

zak S, Rajewsky N and Kadener S. circRNA biogenesis competes with pre-mRNA splicing. Mol Cell 2014; 56: 55-66.
[8] Conn SJ, Pillman KA, Toubia J, Conn VM, Salmanidis M, Phillips CA, Roslan S, Schreiber AW, Gregory PA and Goodall GJ. The RNA binding protein quaking regulates formation of circRNAs. Cell 2015; 160: 1125-1134.
[9] Yan L, Feng J, Cheng F, Cui X, Gao L, Chen Y, Wang F, Zhong T, Li Y and Liu L. Circular RNA expression profiles in placental villi from women with gestational diabetes mellitus. Biochem Biophys Res Commun 2018; 498: 743-750.
[10] Luan J, Jiao C, Kong W, Fu J, Qu W, Chen Y, Zhu X, Zeng Y, Guo G, Qi H, Yao L, Pi J, Wang L and Zhou H. circHLA-C plays an important role in lupus nephritis by sponging miR-150. Mol Ther Nucleic Acids 2018; 10: 245-253.
[11] Zhu LP, He YJ, Hou JC, Chen X, Zhou SY, Yang SJ, Li J, Zhang HD, Hu JH, Zhong SL, Zhao JH and Tang JH. The role of circRNAs in cancers. Biosci Rep 2017; 37.
[12] Yang C, Yuan W, Yang X, Li P, Wang J, Han J, Tao J, Li P, Yang H, Lv Q and Zhang W. Circular RNA circ-ITCH inhibits bladder cancer progression by sponging miR-17/miR-224 and regulating p21, PTEN expression. Mol Cancer 2018; 17: 19.
[13] Guo W, Zhang J, Zhang D, Cao S, Li G, Zhang S, Wang Z, Wen P, Yang H, Shi X, Pan J and Ye H. Polymorphisms and expression pattern of circular RNA circ-ITCH contributes to the carcinogenesis of hepatocellular carcinoma. Oncotarget 2017; 8: 48169-48177.
[14] Zhang S, Zeng X, Ding T, Guo L, Li Y, Ou S and Yuan H. Microarray profile of circular RNAs identifies hsa_circ_0014130 as a new circular RNA biomarker in non-small cell lung cancer. Sci Rep 2018; 8: 2878.
[15] Jiang MM, Mai ZT, Wan SZ, Chi YM, Zhang X, Sun BH and Di QG. Microarray profiles reveal that circular RNA hsa_circ_0007385 functions as an oncogene in non-small cell lung cancer tumorigenesis. J Cancer Res Clin Oncol 2018; 144: 667-674.
[16] Yao JT, Zhao SH, Liu QP, Lv MQ, Zhou DX, Liao ZJ and Nan KJ. Over-expression of CircRNA_100876 in non-small cell lung cancer and its prognostic value. Pathol Res Pract 2017; 213: 453-456.
[17] Han D, Li J, Wang H, Su X, Hou J, Gu Y, Qian C, Lin Y, Liu X, Huang M, Li N, Zhou W, Yu Y and Cao X. Circular RNA circMTO1 acts as the sponge of microRNA-9 to suppress hepatocellular carcinoma progression. Hepatology 2017; 66: 1151-1164.
[18] Guo Y, Ying L, Tian Y, Yang P, Zhu Y, Wang Z, Qiu F and Lin J. miR-144 downregulation increases bladder cancer cell proliferation by targeting EZH2 and regulating Wnt signaling. FEBS J 2013; 280: 4531-4538.
[19] Pan Y, Zhang J, Fu H and Shen L. miR-144 functions as a tumor suppressor in breast cancer through inhibiting ZEB1/2-mediated epithelial mesenchymal transition process. Onco Targets Ther 2016; 9: 6247-6255.
[20] Ma X, Yang X, Bao W, Li S, Liang S, Sun Y, Zhao Y, Wang J and Zhao C. Circular RNA circMAN2B2 facilitates lung cancer cell proliferation and invasion via miR-1275/FOXK1 axis. Biochem Biophys Res Commun 2018; 498: 1009-1015.
[21] Wang X, Zhu X, Zhang H, Wei S, Chen Y, Chen Y, Wang F, Fan X, Han S and Wu G. Increased circular RNA hsa_circ_0012673 acts as a sponge of miR-22 to promote lung adenocarcinoma proliferation. Biochem Biophys Res Commun 2018; 496: 1069-1075.
[22] Hansen TB, Jensen TI, Clausen BH, Bramsen JB, Finsen B, Damgaard CK and Kjems J. Natural RNA circles function as efficient microRNA sponges. Nature 2013; 495: 384-388.
[23] Yao Q, Gu A, Wang Z and Xue Y. MicroRNA-144 functions as a tumor suppressor in gastric cancer by targeting cyclooxygenase-2. Exp Ther Med 2018; 15: 3088-3095.
[24] Tao P, Wen H, Yang B, Zhang A, Wu X and Li Q. miR-144 inhibits growth and metastasis of cervical cancer cells by targeting VEGFA and VEGFC. Exp Ther Med 2018; 15: 562-568.
[25] Gao F, Wang T, Zhang Z, Wang R, Guo Y and Liu J. Regulation of activating protein-4-associated metastases of non-small cell lung cancer cells by miR-144. Tumour Biol 2015; [Epub ahead of print].
[26] Han S, Zhu J and Zhang Y. miR-144 potentially suppresses proliferation and migration of ovarian cancer cells by targeting RUNX1. Med Sci Monit Basic Res 2018; 24: 40-46.
[27] Ren K, Liu QQ, An ZF, Zhang DP and Chen XH. MiR-144 functions as tumor suppressor by targeting PIM1 in gastric cancer. Eur Rev Med Pharmacol Sci 2017; 21: 3028-3037.
[28] Sun J, Shi R, Zhao S, Li X, Lu S, Bu H, Ma X and Su C. E2F8, a direct target of miR-144, promotes papillary thyroid cancer progression via regulating cell cycle. J Exp Clin Cancer Res 2017; 36: 40.
[29] Wang W, Zhou X and Wei M. MicroRNA-144 suppresses osteosarcoma growth and metastasis by targeting ROCK1 and ROCK2. Oncotarget 2015; 6: 10297-10308.
[30] Chen S, Li P, Li J, Wang Y, Du Y, Chen X, Zang W, Wang H, Chu H, Zhao G and Zhang G. MiR-144 inhibits proliferation and induces apoptosis and autophagy in lung cancer cells by targeting TIGAR. Cell Physiol Biochem 2015; 35: 997-1007.

[31] Wang Y, Zhang Y, Yang T, Zhao W, Wang N, Li P, Zeng X and Zhang W. Long non-coding RNA MALAT1 for promoting metastasis and proliferation by acting as a ceRNA of miR-144-3p in osteosarcoma cells. Oncotarget 2017; 8: 59417-59434.

[32] Li H, Shi H, Gao M, Ma N and Sun R. Long non-coding RNA CASC2 improved acute lung injury by regulating miR-144-3p/AQP1 axis to reduce lung epithelial cell apoptosis. Cell Biosci 2018; 8: 15.

[33] Cao J, Han X, Qi X, Jin X and Li X. TUG1 promotes osteosarcoma tumorigenesis by upregulating EZH2 expression via miR-144-3p. Int J Oncol 2017; 51: 1115-1123.